A QUANTITATIVE STEREOLOGICAL DESCRIPTION OF THE ULTRASTRUCTURE OF NORMAL RAT LIVER PARENCHYMAL CELLS

ALDEN V. LOUD

From the Department of Pathology, College of Physicians and Surgeons, Columbia University, New York 10032

ABSTRACT

The principles of stereology have been applied to a morphometric analysis of parenchymal cells from the peripheral, midzonal, and central regions of normal rat liver lobules. The fractional volumes of cytoplasm occupied by mitochondria, peroxisomes, lysosomes, lipid, and glycogen have been determined. The surface densities of smooth- and rough-surfaced endoplasmic reticulum and of mitochondrial envelope and cristae have also been measured. The average number and dimensions of mitochondria and peroxisomes have been evaluated. By the use of an independent measurement of the average cytoplasmic volume, these data have been expressed as the actual volumes, areas, and numbers *per cell* in the different parts of the hepatic lobule. Similarly, the volumes of the envelope, cristae, and matrix compartments and the area of cristae membranes have been calculated for the average-sized mitochondrion in each lobular zone. Structural homogeneity is found in over 80% of normal rat liver parenchymal cells, with most of the significant differences being confined to those cells immediately surrounding the central veins.

INTRODUCTION

Qualitative aspects of the ultrastructure of the parenchymal cells in rat liver have been the subject of numerous investigations and several reviews (1–4). These studies have described the structural characteristics of cytoplasmic organelles and, in conjunction with cytochemical and biochemical techniques, have established many of their associated functional roles in cell physiology (5–9). Hepatic parenchymal cells are not entirely homogeneous with respect to their structure, however, since heterogeneities among the cells of the liver lobule have long been known with respect to mitochondrial form (10, 11) and glycogen deposition (12). Histochemical studies have shown specific patterns of enzyme localization in the central and peripheral zones of hepatic lobules (13, 14) and electron microscopy also has revealed specific sublobular changes in ultrastructure under experimental conditions (15–19). However, no systematic comparison of cytoplasmic ultrastructure in the various zones of hepatic lobules has been made.

The techniques of quantitative stereology (20) constitute another approach to the description of cellular and tissue structure. At the level of light microscopy, liver morphology has been quantitatively studied with respect to nuclear:cytoplasmic ratios (21, 22) and the distribution of nuclear diameters and cell types (23). After the demonstration that quantitative electron microscopy could provide a significant evaluation of cytoplasmic membranes (24), measurements of the area of total endoplasmic reticulum (smooth- and rough-surfaced combined) and the average di-

mensions of mitochondria and peroxisomes (microbodies) were accomplished in randomly selected normal rat liver cells (24, 25). The present investigation extends this earlier work and deals particularly with the quantitative ultrastructure of normal rat liver parenchymal cells characteristic of the peripheral, midzonal, and central regions of hepatic lobules. In addition, the separately determined quantities of smooth-surfaced endoplasmic reticulum, rough-surfaced endoplasmic reticulum, glycogen, and the internal composition of mitochondria have been evaluated in terms of the average volume of cytoplasm per mononucleate cell. These results provide a basis at the cellular level for the quantitative comparison of normal and experimentally altered liver cells (26, 27).

MATERIALS AND METHODS

Tissue samples were taken from the left lateral lobes of the livers of three 5-month-old female Columbia-Sherman rats. The rats had been fed laboratory chow ad libitum until sacrificed between 10:00 and 11:00 a.m. Each lobe was quickly immersed in 6.25% glutaraldehyde fixative in 0.075 M phosphate buffer at pH 7.4. The lobes were first cut into long slices to facilitate removal of marginal and surface cells and then the remaining tissue was minced into several hundred small blocks. The tissue was transferred to fresh fixative for 3 hr, washed thoroughly with buffer, fixed an additional 3 hr in 2% OsO_4 with added sucrose in pH 7.4 veronal acetate buffer, dehydrated with acetone, and finally embedded in Araldite resin.

1-μ-thick sections of plastic embedded liver tissue were cut from twenty-five blocks from each rat and stained with toluidine blue for light microscopy. Light micrographs of these sections were taken for the purpose of measuring the average cell size and nuclear diameter of hepatic parenchymal cells. These sections were also used for locating specific sublobular zones of hepatic lobules in the cut surface of the tissue blocks. Small areas were selected, trimmed, and silver-to-gray thin sections were cut for electron microscopy. Centrilobular areas were trimmed so that they included part of a central vein; peripheral areas included a recognizable portion of the portal triad, and midzonal areas were trimmed at least six cell diameters away from either lobular extreme. Sections for electron microscopy were stained with uranyl acetate and lead citrate.

Electron micrographs of thin sections were taken at three levels of magnification in a Siemens-Elmiskop I electron microscope. Low magnification pictures, × 600–800, were used for recording the position of parenchymal cells with respect to the structures which define the hepatic lobules. Profiles of cells adjacent to a portal triad were designated P-1, those in the next tier of cells, P-2, etc. Similarly, C-1 cells were located next to a central vein, C-2 cells were one cell removed, and so forth. Midzonal cells were identified, as described above, by the areas selected for final trimming of the tissue block.

Electron micrographs used for the general characterization of cytoplasmic structure were taken at × 2500, a magnification low enough to record whole cell cross-sections, but high enough to permit the measurement of membranes and particulate components. Since it was desirable to have as representative a sampling of cells as possible, attempts were made to minimize any subjective influence in the selection of cells in the electron microscope. First, the choice of cells was limited by keeping the area of tissue sections very small, less than 0.01 mm^2. Insofar as possible, no micrographs were taken of cells showing such technical artifacts as knife marks, chatter, compression, dirt, or other contamination. The cells that were micrographed had been clearly identified with respect to their location in the lobule, but no condition of cytoplasmic appearance or the presence of a nucleus in the section (present in about one-half the cells) was imposed. Although each micrograph showed predominantly one cell, adjacent portions of other cells were usually included.

Smaller areas of parenchymal cell cytoplasm were micrographed at × 10,000 so that measurements could be obtained of the internal composition of mitochondria. The intralobular location of each cell was noted, and mitochondria occurring singly and in clusters were sampled in all cytoplasmic sites: perinuclear, pericanalicular, adjacent to the sinusoidal pole, among glycogen aggregates or surrounded by endoplasmic reticulum.

Measurements of cellular, cytoplasmic, and mitochondrial structure were all carried out with the use of 8-×-10-in enlarged prints of the micrographs. A square grid of white lines was superimposed on each picture (see Figs. 1, 3–8) by lengths of 7-mil stainless steel wire attached to the frame of the enlarging easel. Light micrographs were enlarged to × 1000 and electron micrographs were enlarged fivefold to final magnifications of × 12,500 and 50,000. Since quantitative measurements require accurate knowledge of the final image magnification, frequent calibration checks were made on the microscopes and enlarging equipment. All micrographs were taken on polyester base film (28), which has high dimensional stability. Repeated measurements of magnification, in agreement with the findings of Bahr and Zeitler (29), were reproducible within a range of 1.5%.

QUANTITATIVE STEREOLOGICAL MEASUREMENTS

The techniques and basic considerations of morphometric analysis, or quantitative stereology,

of biological materials have been discussed in several recent papers (20, 25, 30). The underlying principle is that quantitative information about the composition of three-dimensional tissue can be calculated from measurements derived from a two-dimensional representation of the tissue, such as a micrograph. Thus, component volumes in a tissue appear as areas in cross-section, surfaces appear as lines, and lines appear as points. It is usually more convenient to measure areas in a micrograph by superimposing an array of sampling lines or points and measuring the length or number, respectively, of these lines or points that overlie the specific area. This method is summarized in the principles of Delesse (31), Rosiwal (32), and Glagolev (33): that the fractional volume occupied by a component is equal to its fractional area in a random cross-section, or the fractional length of random penetrating lines, or the fraction of random points enclosed within it:

$$V_{Vi} = A_{Ai} = L_{Li} = P_{Pi} \qquad \{1\}$$

(The notation used here is given by Weibel et al., 30.)

Lipoprotein membranes within a tissue, such as the membranes of the endoplasmic reticulum and the enclosing envelopes of cells, nuclei, and cytoplasmic organelles, are seen as lines in cross-sections. The length of these lines per unit area of micrograph is proportional to the area of the membranes per unit volume (34, 35). The length of membrane profile is easily measured by counting the number of its intersections with an array of superimposed lines. The area of membrane included in a unit test volume is termed the surface density, S_{Vi} (30), and is given by

$$S_{Vi} = 2N_{Li} \qquad \{2\}$$

where N_{Li} is the number of membrane intersections per unit length of sampling line. Since biological membranes have a finite thickness, the membrane area calculated by formula {2} is equivalent to the surface area on each side of the membrane.

The number of a given particle, for example, nuclei, mitochondria, lysosomes, *etc.*, per unit volume of tissue, N_{Vi}, is proportional to the number of transections of such structures seen per unit area of a tissue section, N_{Ai}:

$$N_{Vi} = N_{Ai}/\bar{D}_i \qquad \{3\}$$

(36). $\bar{D}_i$ is defined as the mean tangent diameter of the particle i and, for a population of uniform spheres, is simply equal to their diameter. In the present study, hepatic parenchymal cell nuclei have been enumerated in light micrographs and peroxisomes enumerated in electron micrographs on the assumption that both these bodies are essentially spherical. If the parameter N_V has only a fractional value per unit volume, its descriptive significance may not be readily apparent. In such cases, it may be convenient either to increase the size of the volume unit to include at least one particle, or to use the reciprocal value, $1/N_V$, which gives the average number of volume units containing a single particle.

These three simple basic mathematical formulations of quantitative stereology assume that the representative sections are not only randomly oriented but also are of negligible thickness. Equation {3} has been extended by Elias et al. (37) to include the effect of a finite section thickness, t:

$$N_V = N_A/(\bar{D} + t) \qquad \{4\}$$

With thickness, however, it is also necessary to consider the perpendicular distance p that a particle must penetrate into a section before it is visible and countable. The general expression, analogous to that derived for spheres (38, 39) is easily shown to be

$$N_V = N_A/(\bar{D} - 2p + t) \qquad \{5\}$$

Formula {5} is identical to {4} when $p = 0$ and to {3} when $p = t/2$. For electron microscopy, where t is usually assumed to be 0.03–0.06 μ for sections which appear gray by reflected light (40, 41) and the value of p is unknown, these factors are probably not significant for particles greater than 0.5 μ. In light microscopy, on the other hand, section thickness is frequently large compared to the diameter of discernible objects. In the present measurements, even the 1-μ thickness of plastic sections is not negligible when counting 8-μ nuclei. Furthermore, since the smallest nuclear sections seen were approximately 3 μ in diameter, it was concluded that a value of $p = 0.3$ μ was appropriate for the calculation of nuclear numbers.

If the particles to be counted are not spherical, $\bar{D}$ becomes a complicated function of their size, shape, and axial ratio (39, 42). Values for these properties must be assumed or derived from other

kinds of data in order to calculate N_V. In the case of liver cell mitochondria, it was previously shown (25) that these three variables could be eliminated by combining two additional independently measured properties of the particles, V_V and S_V derived from equations {1} and {2}, with the arbitrary assumption that mitochondria have the shape of right circular cylinders. This method has been used in the present study for deriving average values for the length and diameter of the "cylindrical" mitochondria. An average mitochondrial volume, v, was then calculated from these figures and, finally, $N_V = V_V/v$.

SAMPLING

The validity of any statistical description of a tissue is basically dependent on the technique for drawing representative samples of the tissue. Aside from the initial removal of surface and marginal cells, the usual method for processing small blocks for electron microscopy assures the complete randomization of the resulting tissue sections with respect to both their location and orientation within the original organ. The steps taken to promote objectivity of sampling in the electron microscope have been described above.

A total of 90 electron micrographs were measured for the determination of general cytoplasmic composition. These were derived from 45 tissue blocks, with a maximum of three micrographs from any one block. Each sublobular zone was represented by five blocks and 10 micrographs from each of the three rats. Higher magnification electron micrographs used for the analysis of mitochondrial substructure numbered three from each of three blocks from each lobular zone from each animal, i.e., a total of 81. The number of micrographs from specific cell locations, C-1, C-2, etc., were uniformly distributed among all rat livers.

While two-dimensional micrographs are the primary sampling of a solid tissue, the method of taking measurements from these pictures by one-dimensional lines is itself another sampling procedure. Obviously, the larger the sample that is taken, i.e., the more sampling lines or points that are measured and counted, the more accurately a micrograph can be described (43). As Hennig (44) has pointed out, it is inefficient to utilize extra effort for measuring a sample micrograph more accurately than the natural variation inherent in the tissue and cellular structures. Description of the tissue is then to be improved mainly by increasing the number of micrographs. The standard deviation of a random counting sample, such as the count of mitochondrial profiles or the count of membrane-line intersections for endoplasmic reticulum, is given by the square root of the total count collected, $\sqrt{C_i}$. For optimum efficiency, the sample size, C_i, should be adjusted so that $\sqrt{C_i}$ is approximately equal to the standard deviation among the values of C_i obtained from a number of different micrographs from the same population. This condition was utilized in setting up the procedures for the present study. In the tables of results which follow, mean values for tissue characteristics have been calculated from the combined raw data of all micrographs in a given group. Each standard error reported is equal to the standard deviation among the corresponding values calculated independently for each micrograph.

RESULTS

Light Microscopy

Average dimensions of liver parenchymal cells were determined at 1,000-fold magnification in 28 light micrographs of 1-μ-thick Araldite sections, similar to that shown in Fig. 1. First, the average diameter of parenchymal cell nuclei was determined by measuring the diameters of 744 circular nuclear sections. These are plotted as a distribution curve in Fig. 2. The distribution of spherical nuclear diameters was then reconstructed from these data by the method of Bach (45, 46) and is also drawn in Fig. 2. The mean nuclear diameter, d, is 8.1 μ, with a standard deviation of 1.0 μ.

Next, the area of these light micrographs occupied by cross-sections of parenchymal cells was measured by the linear scan technique, and the number of nuclear sections within this area was counted. The ratio of these figures, N_A, is 15.9 nuclei per $10^4\mu^2$ of parenchymal cell cross-section. The number of nuclei per unit volume of parenchymal cells, N_V, was calculated from formula {5} to be 186 nuclei per $10^6\mu^3$. The reciprocal of this figure, parenchymal cell volume per nucleus, is 5400 μ^3. Subtracting the volume of an average nucleus, 280 μ^3, leaves 5100 μ^3 of cytoplasm per nucleus. Except for the abundance of binucleate cells in liver (47), the last figure would represent the average cytoplasmic volume per cell. Nevertheless, because the cell is a fundamental biological

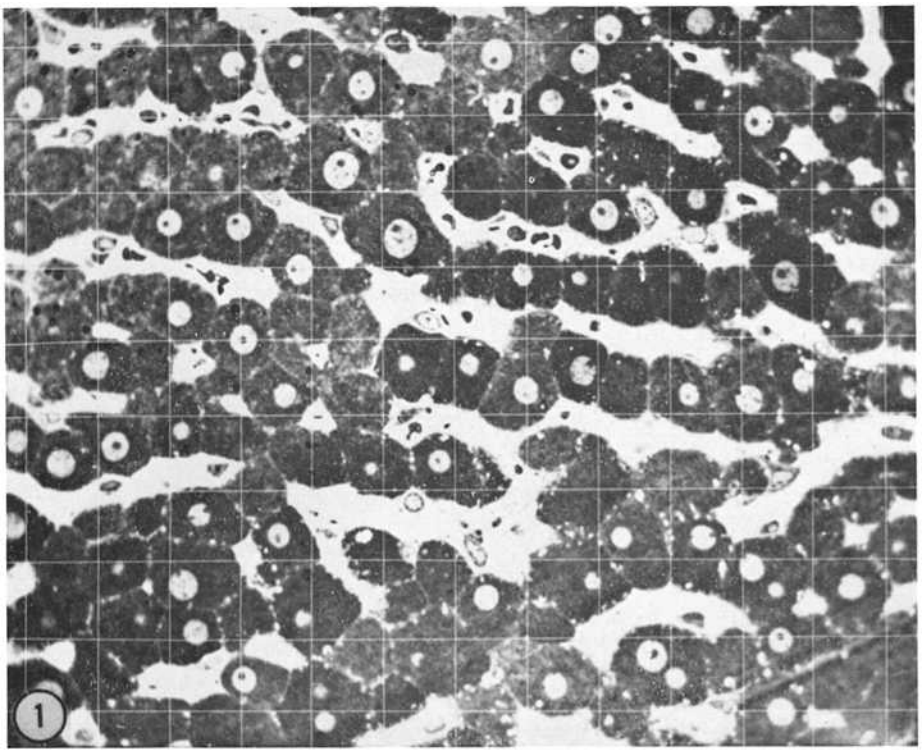

FIGURES 1, and 3–8 are all ×½ reproductions of electron micrographs printed with the superimposed grid used for stereological structural analysis. Fig. 1 is a micrograph of a 1-μ-thick Araldite-embedded section stained with toluidine blue and having an original magnification of 1,000. The original magnification of the electron micrographs in Figs. 3–5 was 12,500 ×, and 50,000 × in Figs. 6–8. Figs. 3 and 6 are electron micrographs of peripheral lobular cells, adjacent to (P-1) and one cell layer removed from (P-2) the portal triad, respectively; Figs. 4 and 7 are midzonal cells; and Figs. 5 and 8 are from centrilobular cells adjacent to a central vein (C-1). The variation in mitochondrial size within the hepatic lobule is particularly noticeable when the extreme centrilobular cells shown in Figs. 5 and 8 are compared with the other figures. Figs. 3–5, × 6,250. Figs. 6–8, × 25,000.

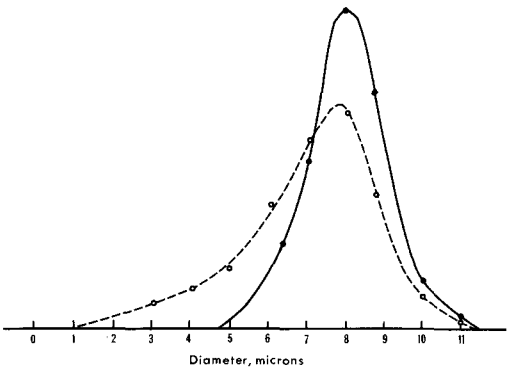

FIGURE 2 This figure shows the distribution curve of actual diameters of nuclear sections (○—○) measured in light micrographs such as Fig. 1. The theoretical distribution of spherical nuclei (●—●) was calculated from the distribution of nuclear sections.

unit, the quantitative electron microscopic data described below and summarized in Tables I-IV have been calculated in terms of 5100 μ^3 and expressed on a "per cell (nucleus)" basis in Table VI. Because binucleate cells appear to have about twice the volume of mononucleate cells (48), the volume "per cell (nucleus)" very nearly approximates that of the average mononucleate cell.

Finally, the size of hepatic parenchymal cells was compared in the different sublobular regions. The maximum and minimum dimensions of approximately 50 cells were measured in each of the peripheral, midzonal, and central zones of liver lobules. The average cell diameter and standard deviation in these zones is 20.8 ± 0.2, 20.8 ± 0.3, and 21.0 ± 0.3 μ, respectively. Thus, no significant difference in average cell size is

demonstrable across the lobules of these normal livers.

Electron Microscopy

A general description of normal liver parenchymal cell cytoplasm as measured in 90 electron micrographs at a magnification of ×12,500 is shown in Tables I, II, and III. The columns in these Tables are arranged to show progressive changes across the hepatic lobule in the functional direction of blood flow from the extreme peripheral cells, P-1, to the innermost C-1 cells. The middle column represents the bulk, about 60%, of the lobular cells, which are here classified as midzonal. Data from the three columns of peripheral cells and from the three columns of central cells, each group representing about 20% of the lobular cells, are combined in the extreme left and right columns, respectively, for the facilitation of comparisons between these zones. Approximately "typical" cells from the peripheral, midzonal, and central regions are illustrated in Figs. 3–5 as they appeared with the superimposed grid of sampling lines.

The top row in Table I shows the number of micrographs analyzed for each sublobular zone and the breakdown for specific cell positions in the peripheral and central regions of the lobules. The total cross-sectional area of parenchymal cell cytoplasm examined in each of these sites is listed next. The remainder of Table I shows the mean percentage and standard error of cytoplasmic volume occupied by mitochondria, peroxisomes (microbodies), lysosomes, lipid, glycogen, and other components. Mitochondria, peroxisomes, and lipid were identified by their characteristic structure and electron opacity. Because of their multiplicity of forms, ranging from autophagic vacuoles to residual bodies (8), all other discrete membrane-bounded bodies were classified as lysosomes. Glycogen in these stained sections appears as very dense particulates measuring approximately 200–400 A in diameter, arranged singly or in clusters (49). Rosettes of glycogen are frequently surrounded by a clear margin about 0.05 μ wide (See Fig. 7). In the process of measuring the volume fraction of cytoplasm occupied by glycogen this clear region was assumed to be part of the glycogen space and was so included. The effect of this assumption is to put all dense glycogen particles separated by less than 0.1 μ into confluence and, thus, permit extended fields of particles to be measured as a continuous zone of glycogen.

Mitochondria occupy nearly 20% of the volume of most liver parenchymal cells. This percentage is significantly lower ($p < 0.001$) only in the centrilobular zone, and particularly in the first two layers of cells surrounding the central vein. Qualitatively, the mitochondria in these cells appear smaller but more numerous (Fig. 5). The volume fraction of peroxisomes is less than 3% in all cells and less than 2% in most. Only the extreme centrilobular cells have a significantly larger ($p < 0.005$) bulk of peroxisomal material than the rest of the lobule. The total sample of lysosomes and lipid, which together account for less than 1% of cytoplasmic volume, is not sufficient to indicate any trends in their sublobular distribution in these normal rats.

Glycogen was found to occupy about the same fraction of parenchymal cell cytoplasm as mitochondria, but this volume relationship is certainly not a constant characteristic of liver cells. If the rats had been sacrificed later in their diurnal feeding cycle, for example, all liver cells, especially those nearer the central veins would have shown considerably less glycogen (12). Nevertheless, the finding of nearly equal concentrations of glycogen in cells from all parts of the hepatic lobule shortly after a night of ad libitum feeding suggests that the measured levels are probably close to the saturation value for these cells. It is not apparent from the quantitative data, but centrilobular glycogen is generally dispersed in small isolated rosettes scattered throughout the cytoplasm and is often closely associated with membranes of smooth-surfaced endoplasmic reticulum (Fig. 8). Glycogen in peripheral cells tends to occur in larger aggregates which are often gathered into broad areas having significantly fewer associated smooth membranes (Fig. 6). Midzonal cells exhibit both forms of glycogen dispersal and appear truly intermediate.

The membrane areas of mitochondrial envelope and endoplasmic reticulum calculated by means of formula {2} are shown in Table II. The area of mitochondrial envelope was measured relative to mitochondrial volume by dividing the surface density of envelope membrane in the cytoplasm by the volume fraction of mitochondria. Thus, the figures in the top row of Table II give the average surface-to-volume ratio for these organelles. The higher ratios in centrilobular cells ($p < 0.001$) reflect the smaller size and elongated shape of the mitochondria in this zone. The surface-to-volume ratio for midzonal mitochondria

TABLE I

Volume Fraction of Cytoplasmic Components

	All peripheral cells	P-1	P-2	P-3,4	All midzonal cells	C-3,4	C-2	C-1	All central cells
Number of micrographs	30	12	8	10	30	8	10	12	30
Total area of cytoplasm (μ^2)	8754	3386	2556	2812	8592	2399	2985	3579	8963
% Cytoplasmic volume									
Mitochondria	19.8	18.6	19.9	21.1	19.1	15.2	13.0	12.0	12.9
(Standard error)	(0.6)	(0.8)	(1.5)	(0.9)	(0.8)	(0.3)	(0.5)	(0.5)	(0.4)
Peroxisomes	1.4	1.3	1.6	1.2	1.4	1.5	1.9	2.4	2.1
(Standard error)	(0.1)	(0.2)	(0.2)	(0.2)	(0.2)	(0.2)	(0.2)	(0.3)	(0.2)
Lysosomes	0.3	0.3	0.2	0.3	0.3	0.3	0.5	0.3	0.4
(Standard error)	(0.05)	(0.09)	(0.05)	(0.08)	(0.07)	(0.07)	(0.12)	(0.09)	(0.06)
Lipid bodies	0.3	0.2	0.3	0.4	0.2	0.2	0.2	0.2	0.2
(Standard error)	(0.12)	(0.09)	(0.33)	(0.20)	(0.08)	(0.06)	(0.08)	(0.09)	(0.05)
Glycogen	20.3	23.0	21.0	16.5	17.4	16.9	15.1	19.5	16.8
(Standard error)	(1.3)	(1.7)	(2.4)	(2.2)	(1.3)	(1.6)	(1.2)	(2.4)	(1.3)
Other	58.9	56.6	57.0	69.5	61.6	65.9	69.3	65.6	67.6
(Standard error)	(1.5)	(1.6)	(2.5)	(3.0)	(1.4)	(2.2)	(0.8)	(2.7)	(1.2)

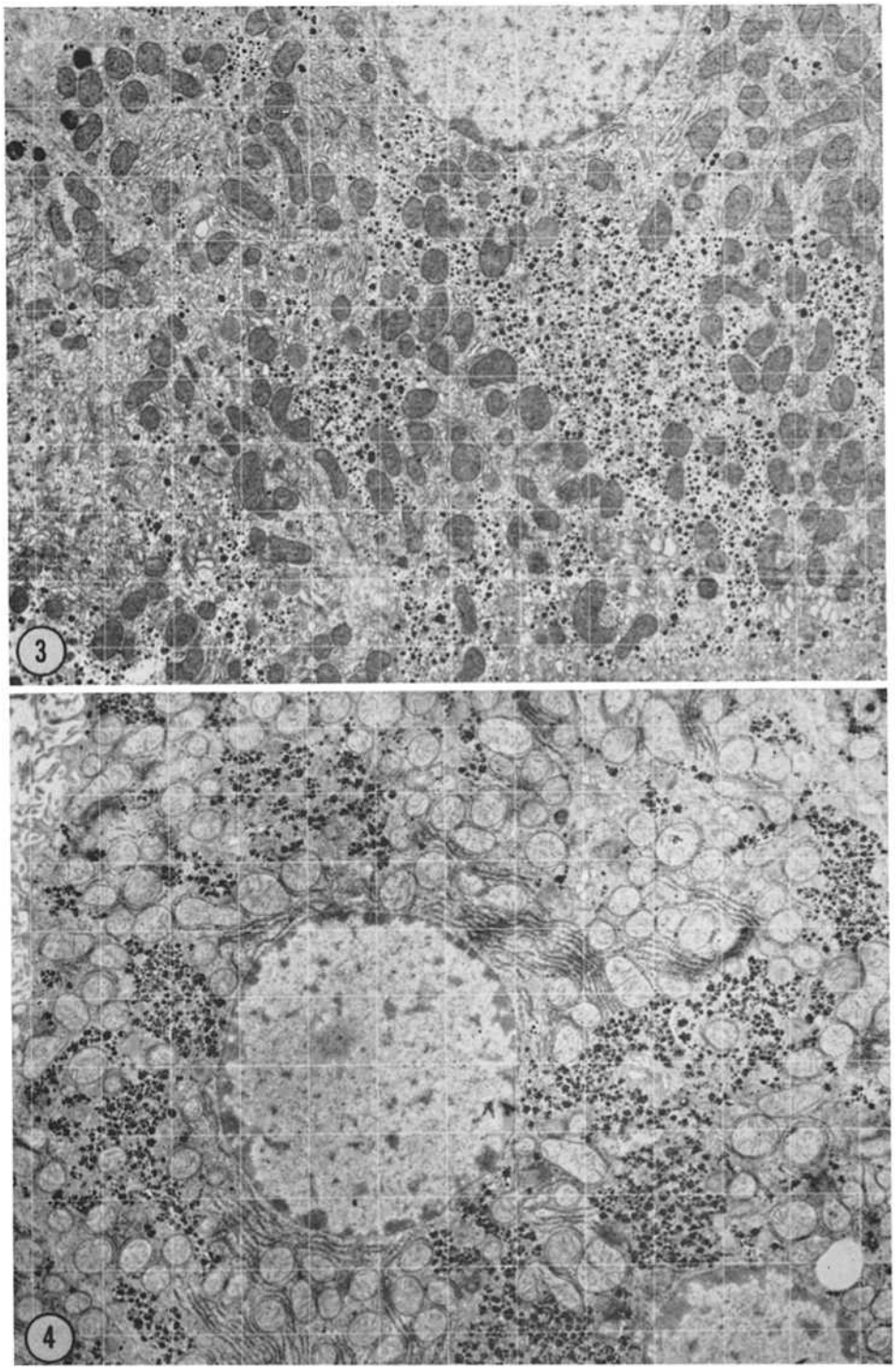

FIGURE 3 Peripheral lobular cell adjacent to a portal triad (P-1).

FIGURE 4 Midzonal cell.

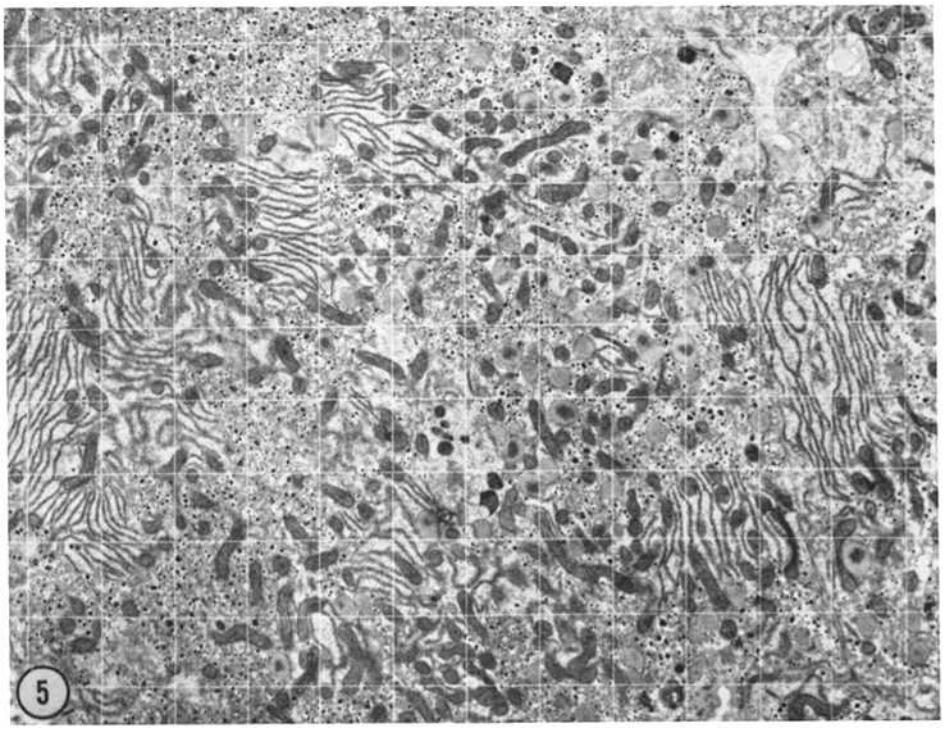

FIGURE 5 Centrilobular cell adjacent to a central vein (C-1).

is also significantly greater ($p < 0.01$) than that for peripheral cells.

The membrane areas of endoplasmic reticulum shown in Table II are expressed per unit volume of the whole cytoplasm. At low magnification, rough-surfaced endoplasmic reticulum appears in higher contrast to the cytoplasmic ground substance and is almost entirely distributed in broad parallel arrays of flattened cisternae. Smooth-surfaced endoplasmic reticulum is generally found in Golgi regions and appears as widely dispersed small vesicles often associated with glycogen deposits. There is relatively little intermixing of the regions of the granular and agranular membranes. The quantitative results show the agranular membranes to be significantly more abundant in centrilobular cells ($p < 0.005$) than in midzonal and peripheral regions of the hepatic lobule. This difference is accounted for principally by the membranes associated with glycogen particles in the two layers of cells most closely surrounding the central vein. The granular reticulum is dispersed without significant differences in its cytoplasmic concentration in all parts of the lobule. Rough-surfaced membranes have approximately 50% more area than smooth-surfaced membranes in cells from all lobular regions, except in those cells immediately adjacent to a central vein where the amounts of both varieties of membrane are nearly equal.

The size of the statistical samples on which the above calculations of surface densities are based is indicated in the lower part of Table II as the total number of membrane-line intersections that were counted. In so large a sample, it can be assumed that these membranes, which occur at all angles within liver cells, are completely randomly oriented within the tissue sections. Most membranes, therefore, lie in the sections at oblique angles to the plane of sectioning. It is a commonly observed phenomenon in electron microscopy, first described by Williams and Kallman (50), that biological membranes sectioned or observed at increasing angles of tilt first broaden, then become indistinct, and, finally, are undetectable. This effect is least in the thinnest sections, but it still precludes an absolute count of all membrane profiles present per unit area of section.

TABLE II

Areas of Mitochondrial Envelope and Endoplasmic Reticulum Membrane

	All peripheral cells	P-1	P-2	P-3,4	All midzonal cells	C-3,4	C-2	C-1	All central cells
μ^2 Mitochondrial envelope									
μ^3 Mitochondria	7.64	7.49	7.74	7.72	8.96	10.6	13.1	14.6	12.8
(Standard error)	(0.15)	(0.25)	(0.34)	(0.22)	(0.49)	(0.4)	(0.5)	(0.5)	(0.4)
μ^2 Endoplasmic reticulum									
μ^3 Cytoplasm									
Smooth surfaced	2.06	2.12	1.83	2.18	2.22	2.51	2.70	3.33	2.82
(Standard error)	(0.12)	(0.20)	(0.17)	(0.22)	(0.17)	(0.22)	(0.17)	(0.22)	(0.13)
Rough surfaced	3.25	3.26	2.93	3.51	3.32	3.61	3.64	3.49	3.49
(Standard error)	(0.15)	(0.26)	(0.22)	(0.25)	(0.13)	(0.29)	(0.32)	(0.20)	(0.16)
Total intersections counted									
Mitochondrial envelope	8294	2989	2374	2931	8967	2475	3186	3650	9311
Smooth endoplasmic reticulum	11223	4522	2810	3891	12277	3894	5056	6968	15918
Rough endoplasmic reticulum	17762	6931	4517	6314	18330	5519	6834	7276	19629

The loss of membrane images resulting from oblique sectioning has recently been investigated quantitatively (51). It was found that membranes tend to "disappear" rather abruptly when tilted more than about 60° from the direction of the electron beam. Therefore, approximately one-third of randomly positioned membranes will be so oriented in normally observed sections. For this reason, it is appropriate to increase all intersection counts of random membranes by 50 % in order to correct for the membranes that are present in sections, but invisible in the electron micrographs. In this report, such a correction has been applied only to certain calculations presented in the summaries indicated by an * in Tables V and VI. It should be noted that, as membrane counting is practiced in this laboratory, the above correction is applicable to measurements of endoplasmic reticulum and mitochondrial cristae (see Table IV), but not to the figures for mitochondrial envelope. In the former instances, counts of membrane intersections have been based entirely on the visibility of the membrane profile itself at the point where it crossed the sampling line. The same is generally true for mitochondria except that in nearly tangential sections, where the organelle is still easily identified by its internal structure, two intersection counts were routinely recorded for the envelope membrane even though its profile was not always clearly visible.

The upper three rows in Table III indicate the total number of transections of mitochondria, peroxisomes, and lysosomes counted in the measured areas of cytoplasm. The number of each of these organelles per unit area of cytoplasmic cross-section is greatest in centrilobular cells and decreases toward the periphery. The particle counts for mitochondria were combined as previously described (25) with the figures for their volume fraction (see Table I) and surface-to-volume ratio (see Table II) so that their average diameter, length, volume, and number per unit volume of cytoplasm recorded in Table III could be obtained. The counts of peroxisomes were combined with the measurements of their cytoplasmic volume fraction by the method of Weibel and Gomez (42) to yield figures for their average diameter, volume, and number per unit volume of cytoplasm as shown in the lower section of Table III. The counts of lysosomes suggest a trend toward greater numbers of these particles in more central portions of the hepatic lobule, in agreement with the observation of Novikoff and Shin (52). The sparsity and irregular shape of lysosomes and their small volume fraction in cytoplasm, however, provide insufficient data on which to base quantitative conclusions concerning the distributions of lysosomal size and number.

It can be seen in Table III that average mitochondria are shorter and larger in diameter toward the periphery of the lobule, and become progressively longer and thinner towards the center, as seen particularly in the C-1 cells. Average length: diameter ratios for peripheral, midzonal, and central cell mitochondria are 7, 9, and 16 respectively. Furthermore, the average volume of peripheral cell mitochondria is more than double that of centrilobular mitochondria, while those in midzonal cells are intermediate in size. Although the volume fraction of mitochondria is least in centrilobular cells, the relative size of individual particles is still smaller, with the result that central cells have the greatest number of mitochondria per unit volume of cytoplasm.

The average diameters and volumes calculated for peroxisomes show some variation in Table III. Although central and midzonal particles are not significantly different, peripheral peroxisomes have a greater diameter than those in midzonal cells at a 5% level of significance. In contrast, the peroxisomes in control animals from a similar quantitative study, in which the effect of cortisone administration on the ultra-structure of rat liver was measured (26), did not show significant differences in their diameters in the sublobular zones. Thus, it appears that present data do not establish any sublobular size differences in hepatic peroxisomes.

Quantitative measurements of intramitochondrial structure derived from 81 higher magnification electron micrographs (×50,000), typified by those in Figs. 6–8, are summarized in Table IV. At higher magnifications, the diffuseness of the edges of obliquely sectioned membranes is much more evident, and it is frequently difficult to decide the precise thickness of paired membranes like those in mitochondrial envelope and cristae folds. Consequently, the simplest basis of decision was accepted, namely, to measure structures between their outermost limits of visible density. In this regard, Weibel et al. (30) have pointed out the importance of using only the thinnest sections in high magnification measurements in order to avoid a systematic overestimation of volume fractions.

Total mitochondrial volume was subdivided into three parts: envelope, cristae, and matrix. The volume fraction of mitochondrial envelope

TABLE III

Number and Dimensions of Mitochondria and Peroxisomes (Microbodies)

	All peripheral cells	P-1	P-2	P-3,4	All midzonal cells	C-3,4	C-2	C-1	All central cells
Number particles counted									
Mitochondria	4014	1476	1153	1385	4889	1590	2164	2622	6376
Peroxisomes	506	185	160	161	634	169	300	415	884
Lysosomes	160	60	51	49	264	67	135	116	318
Mitochondrial dimensions									
Average diameter (μ)	0.562	0.586	0.547	0.554	0.471	0.402	0.314	0.278	0.323
(Standard error)	(0.017)	(0.028)	(0.034)	(0.023)	(0.024)	(0.020)	(0.013)	(0.010)	(0.012)
Average length (μ)	3.85	3.02	4.68	4.01	4.32	3.05	5.81	9.27	5.04
(Standard error)	(0.67)	(1.33)	(1.34)	(0.48)	(0.40)	(0.69)	(3.08)	(2.01)	(1.38)
Average volume (μ^3)	0.954	0.814	1.10	0.967	0.752	0.387	0.448	0.563	0.411
(Standard error)	(0.158)	(0.326)	(0.31)	(0.096)	(0.112)	(0.070)	(0.226)	(0.113)	(0.092)
Average number/100 μ^3 cytoplasm	20.8	22.9	18.1	21.8	25.4	39.3	29.0	21.3	31.4
(Standard error)	(2.6)	(5.3)	(2.8)	(3.5)	(5.0)	(9.3)	(9.7)	(3.2)	(4.4)
Peroxisome dimensions									
Average diameter (μ)	0.676	0.652	0.723	0.626	0.603	0.654	0.603	0.626	0.633
(Standard error)	(0.025)	(0.040)	(0.029)	(0.051)	(0.022)	(0.019)	(0.030)	(0.026)	(0.016)
Average volume (μ^3)	0.162	0.145	0.198	0.128	0.114	0.147	0.115	0.129	0.133
(Standard error)	(0.021)	(0.040)	(0.023)	(0.034)	(0.012)	(0.012)	(0.019)	(0.019)	(0.011)
Average number/100 μ^3 cytoplasm	8.7	9.0	8.1	9.4	12.2	10.2	16.6	18.7	15.8
(Standard error)	(0.8)	(1.1)	(1.5)	(1.4)	(1.7)	(1.8)	(2.0)	(2.9)	(1.5)

TABLE IV

Intramitochondrial Structure

	All peripheral cells	P-1	P-2	P-3,4	All midzonal cells	C-3,4	C-2	C-1	All central cells
Number of micrographs	27	9	9	9	27	9	9	9	27
Total area of mitochondria (μ^2)	123.2	37.1	44.0	42.4	123.0	29.7	25.1	24.8	80.3
% Mitochondrial volume									
Envelope	13.8	13.5	13.9	13.9	16.1	19.1	23.6	26.3	23.0
(Standard error)	(0.2)	(0.4)	(0.3)	(0.4)	(0.5)	(0.8)	(1.2)	(0.7)	(0.8)
Cristae	25.5	25.0	25.6	25.9	27.6	26.3	23.8	23.8	24.8
(Standard error)	(0.5)	(0.9)	(1.0)	(0.7)	(0.6)	(0.8)	(1.2)	(0.6)	(0.6)
Matrix	60.7	61.5	60.5	60.2	56.3	54.6	52.6	49.9	52.2
(Standard error)	(0.5)	(1.0)	(0.9)	(0.8)	(0.8)	(0.9)	(1.4)	(0.8)	(0.7)
Total cristae intersections counted	8283	2561	2839	2883	9290	2326	1947	1836	6109
μ^2 Cristae membrane / μ^3 Mitochondria	21.4	21.9	20.5	21.8	24.3	24.4	24.6	23.5	24.2
(Standard error)	(0.4)	(1.0)	(0.7)	(0.6)	(0.4)	(0.6)	(1.1)	(0.8)	(0.5)
Total dense granules counted	914	303	304	307	816	286	201	207	694
Number dense granules / μ^2 Matrix cross-section	12.2	13.3	11.4	12.0	11.8	17.6	15.2	16.7	16.6
Approximate number dense granules* / μ^3 Matrix	190	200	180	180	180	270	230	260	260

* Calculated by formula $\{5\}$ using $\bar{D} = 0.025\mu$, $p = 0.005\mu$ and $t = 0.05\mu$.

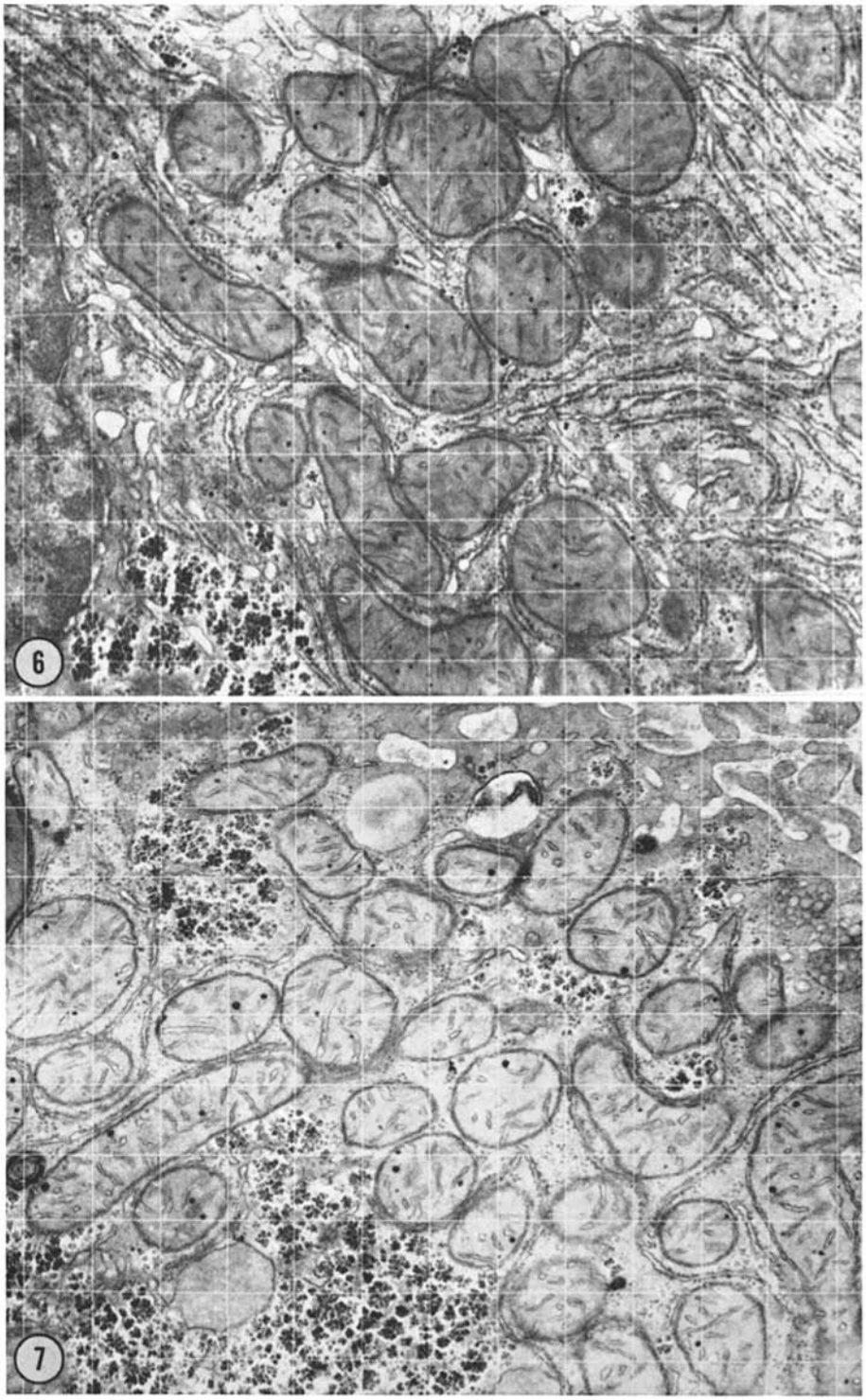

FIGURE 6 Peripheral lobular cell one cell layer removed from portal triad (P-2).

FIGURE 7 Midzonal cell.

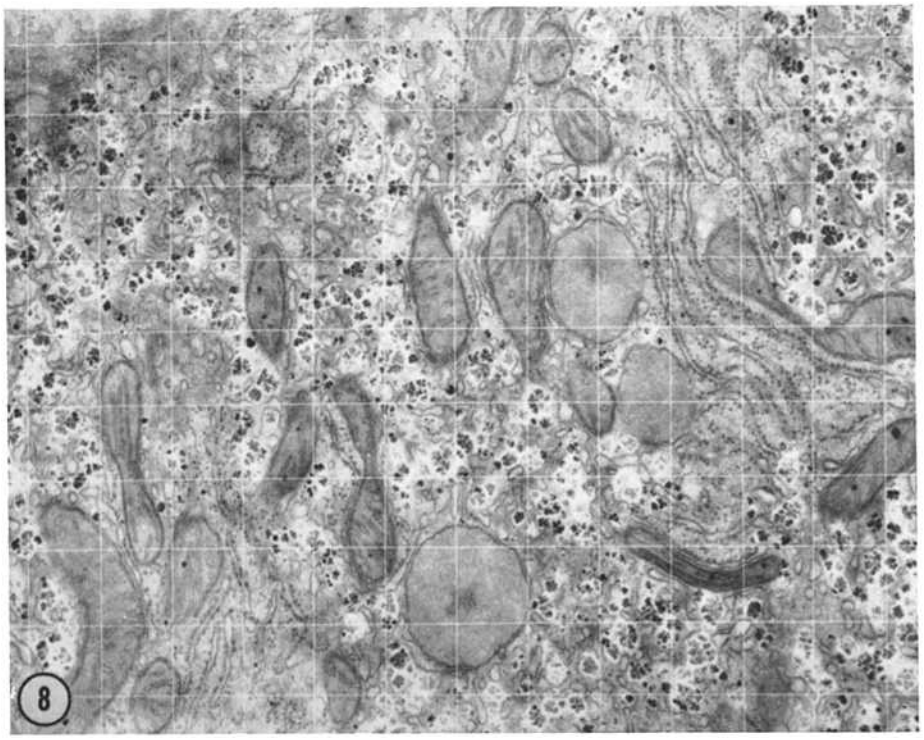

FIGURE 8 Centrilobular cell adjacent to a central vein (C-1).

was calculated by multiplying the surface-to-volume ratios from Table II by an envelope thickness of 0.018 μ (5). This calculation was considered more reliable than direct measurements at × 50,000 because the lower magnification pictures contained more than 16 times as many mitochondrial cross-sections and yielded a smaller statistical error. The volume fraction of cristae describes the volume enclosed inside the outermost visible densities of cristae folds and thus includes both the volume of the membranes and any intracristae space. The matrix volume is then that part of the mitochondrion distinct from envelope and cristae volumes. It is apparent from these results that the envelope comprises a significant fraction of total mitochondrial structure, exceeding an average value of 25% in C-1 cells. The figures also reveal considerable uniformity in the volume per cent of cristae and matrix, despite the more than twofold variation in average mitochondrial size across the hepatic lobule.

The total count of intersections between cristae membranes and sampling lines and the calculated membrane area per unit volume of mitochondria is also shown in Table IV. The latter figures again illustrate the constancy of the internal composition of mitochondria in all parts of the liver lobule. As mentioned above, the number of visible random membrane sections is subject to a correction factor (51) for the effects of oblique orientation of membranes within the tissue sections.

The small dense granules that are commonly observed in matrix space have also been counted in all mitochondrial sections. These totals and the number of granules observed per unit area of matrix are shown in Table IV. Because of the small size of these granules, approximately 250 A in diameter (5), their number per unit volume of matrix cannot be accurately calculated without knowledge of the section thickness in which the counts were made. Unfortunately, it is difficult to determine precisely the thickness of sections used in electron microscopy: it is quite variable. If, for the purpose of making a rough estimate, a section thickness of 500 A is assumed (41), then the approximate values for the number of dense granules per unit volume of mitochondrial matrix are as shown in the last row of Table IV.

Structure in Terms of Biological Units

The techniques of stereology, or morphometric analysis, are fundamentally statistical and geometrical, yielding only average values expressed in geometrical units. Thus, the results tabulated in Tables I–IV are average measures of volume, area, and number *per unit volume*. Biological systems, on the other hand, frequently occur in discrete structural units such as an organism, organ, cell, or mitochondrion. Therefore, it may be more meaningful for morphological comparisons to express these quantitative data in terms of biological rather than geometrical units. The conversion factor from one system of units to the other is simply a figure for the average volume of the biological unit.

Determining the average volume of a biological unit is also a stereological task requiring a sufficiently large random sample of the structure. In general, the magnification that is appropriate for sampling the over-all size of a structure is smaller by about an order of magnitude than the magnification that is convenient for examining its internal composition. Thus, the internal structure of mitochondria (Table IV) has been measured at × 50,000 in about 300 profiles per lobular zone, while the average mitochondrial size was determined from about 5,000 profiles at × 12,500. Similarly, the over-all composition of cytoplasm per zone was measured in micrographs of 30 different cells at × 12,500, but a figure for the average amount of cytoplasm per cell (nucleus) was derived from micrographs of more than 700 cells at × 1000.

Tables V and VI are summary tables showing the structural composition of the average mitochondrion and the average parenchymal cell in each of the principal sublobular zones in normal rat liver. These figures were determined by multiplying the corresponding values per unit volume in the preceding tables by the average volume retabulated at the top of each column. These tables have been simplified by omitting the figures for specific cell sites, which can be calculated in the same manner, and the standard errors, which are related to the values already recorded.

TABLE V

Characteristics of the Average Mitochondrion

	Peripheral cells	Midzonal cells	Central cells
Volume (μ^3)			
Total	0.954	0.752	0.411
Envelope	0.131	0.121	0.094
Cristae	0.243	0.207	0.102
Matrix	0.580	0.424	0.215
Membrane area (μ^2)			
Envelope	7.3	6.7	5.3
Cristae*	30.6	27.4	14.9
Approximate number of dense granules	110	77	55

* These figures, which are obtained by multiplying the measured cristae area per unit volume by the average volume per mitochondrion, have been further increased by 50% to correct for the effect of oblique sectioning on the observability of membrane profiles (51).

TABLE VI

Ultrastructural Composition of Rat Liver Parenchymal Cells Calculated per Average Cell (Nucleus)

	Peripheral cells	Midzonal cells	Central cells
Volume (μ^3)			
Total cytoplasm	5100	5100	5100
Mitochondria	1010	974	658
Envelope	139	157	151
Cristae	257	269	163
Matrix	614	548	344
Peroxisomes	71	71	107
Lysosomes	15	15	20
Lipid	15	10	10
Glycogen	984	887	857
Other	3000	3140	3450
Membrane area (μ^2)			
Smooth endoplasmic reticulum*	15700	16900	21600
Rough endoplasmic reticulum*	24900	25400	26700
Mitochondrial envelope	7720	8720	8420
Mitochondrial cristae*	32400	35500	23900
Number of			
Mitochondria	1060	1300	1600
Peroxisomes	440	620	810

* These figures, which are obtained by multiplying the measured membrane area per unit volume by the average volume per cell, have been further increased by 50% to correct for the effect of oblique sectioning on the observability of membrane profiles (51).

Table V shows the actual volumes of the envelope, cristae, and matrix compartments in average liver mitochondria. The membrane area of envelope is numerically equal to the outer surface area of the mitochondrion. An approximately equal area of inner envelope membrane faces the matrix space, while twice this surface area abuts on any compartment between the envelope membranes. Similarly, the area of cristae membranes can also be interpreted as the surface area on each side of the membrane, that is, the area facing matrix substance and the area lining intracristae compartments. Thus, the total area bounding matrix space is the sum of the envelope and cristae areas, which is four to five times the outer surface area. Because of the limitations discussed above, the figures for the number of dense matrix granules should only be considered as rough estimates.

Since no significant difference could be shown in the average size of parenchymal cells among the lobular zones of rat liver, the figures in Table VI are all proportional to values in Tables I through IV and to the common cytoplasmic volume of 5100 μ^3 per cell (nucleus) measured in these fixed plastic embedded tissues. It is of interest that the total area of cristae membranes exceeds the area of either rough- or smooth-surfaced endoplasmic reticulum in cells of the midzonal and peripheral regions and is essentially equal to these classes of membranes in centrilobular cells. Another noteworthy finding is the rather constant amount of mitochondrial envelope in cells from all zones. A further correlation that may be more than coincidental is the apparent 2:1 ratio of the number of mitochondria and peroxisomes in all groups of liver cells.

One final result of this investigation is the observation that the parenchymal cells of normal rat liver are at least 80% homogeneous with respect to the structural parameters measured here. The groups that have been designated as peripheral and central cells each account for about 20% of the hepatocytes across a lobule, and the midzonal cells comprise the remaining 60%. Cells in all zones show some common structural characteristics, but midzonal and peripheral cells resemble each other in nearly all measurements. Where significant intralobular differences in structure do exist, they are generally confined to one extreme or the other of the lobules, especially to the two or three layers of cells surrounding the central veins.

DISCUSSION

The application of quantitative stereological techniques to a representative sampling of tissue provides a numerical and unequivocal basis for the description of the tissue and for the evaluation of developmental, pathological, or experimental changes. As a statistical method, it affords a continuous means for measuring the variation and significance of accumulating data and a mathematical foundation on which to improve the design of experiments. As a method that deals fundamentally with geometrical abstractions, such as volume, surface, length, etc., it is only supplemental to, but cannot replace, the observations of qualitative morphology. The use of these techniques, however, has become potentially much more important in biology since the electron microscope has revealed the extensive complex of membranes which subdivide cytoplasm into numerous functional compartments whose physiological significance is undoubtedly related to their surface areas and component volumes.

The results presented in this study establish a quantitative structural base line for normal rat liver parenchymal cells. A comparative description of the cells throughout the average hepatic lobule was obtained by appropriate sampling of peripheral, midzonal, and central regions. Furthermore, by combining data from different ranges of magnification, it has been possible to express the results not only in the geometrical term *per unit volume*, but also in the biological unit *per cell (nucleus)*. The qualification "(nucleus)" is a necessary compromise resulting from the large fraction of binucleate cells in the hepatic parenchyma. It is understood that the numerical values per cell (nucleus) refer to that average amount of cytoplasm associated with a single parenchymal cell nucleus and, therefore, are probably very nearly appropriate to the typical mononucleate cell.

Although considerably more complete than previous measurements of cytoplasmic structure in liver parenchymal cells (24, 25), the present description of normal liver is still limited in several ways. Only an early phase of the diurnal glycogen cycle is represented, in which all cells have abundant and nearly equal amounts of glycogen (12). While measurements are reported for all other kinds of membranes, no attempt was made to assay the area of cell surface membrane since this will require a somewhat different and more involved sampling approach. As a description of

liver, these data are incomplete because they include no information concerning the vascular and connective tissues or the large population of Kupffer cells.

The errors in sampling have already been mentioned in regard to the selection of a limited number of tissue blocks and micrographs and in the method of drawing measurements from the micrographs. The principal source of variation in the final results is the natural biological variation occurring among random cell sections. Although this study is based on the examination of the livers from only three rats, no significant differences were found among the results from individual animals. The assumption that mitochondria can be considered as a uniform population of right circular cylinders is clearly an oversimplification. Many normal mitochondria, especially the long curved forms seen in centrilobular cells, and the irregular branched and annulate shapes produced by cortisone administration (26) can appear as two or more profiles in a thin section. This property, impossible for a straight cylinder, leads to an underestimation of the average lengths and volumes of such mitochondria in the final calculations. For a reasonable comparison of different groups of mitochondria, however, the assumed cylindrical shape does provide a basis which utilizes all available quantitative measures of mitochondrial number, volume, and surface area (25). Finally, by the use of the correction factor for the loss of membrane images due to oblique sectioning (51), the figures for the total area of cytoplasmic membrane in cells are significantly improved over previous uncorrected measurements.

The results of this study are in general agreement with other measurements of cytoplasmic ultrastructure in liver parenchymal cells from female rats of different strains (24, 25) and from younger male rats (26). The volume fractions of cytoplasmic organelles, the distribution of mitochondrial sizes, the size of peroxisomes, and the amount of endoplasmic reticulum membrane were all found to be essentially similar.

In general, it is not necessary to carry out such detailed work to establish most comparisons in cytoplasmic morphology. When quantitative observations are available, however, it is often possible to correct interpretations derived from nonquantitative studies. For example, the present data disagree with the contentions that centrilobular cells have fewer microbodies (peroxisomes) than peripheral cells (52) and that rough-surfaced endoplasmic reticulum is less abundant in peripheral cells (53).

It is a common experience in light and electron microscopy that different groups of cells and structures are recognizable by their typical appearance. The ultrastructure of normal liver cell cytoplasm and liver mitochondria, for example, is very characteristic and easily recognized by cytologists. Such constancy of form reflects a dynamic equilibrium within cytoplasm responding to influences of cellular environment, on the one side, and of nuclear directives, on the other. This equilibrium is apparent not only in the spatial arrangement of component structures, but also in their geometric properties of size, shape, volume, surface area, and number. It is in the ability to measure these latter properties that stereological techniques provide a quantitative key to the unique characteristics which differentiate particular cell types and the special form of organelles (54).

The results of the present investigation are an example of the structural equilibria which characterize normal liver parenchymal cells. Thus, 80% of the cells were found to be similar with respect to all of their measured properties. Those that show significant variation tend to be grouped around the central vein. Even there, however, some structural equilibria remain unchanged. All groups of parenchymal cells, regardless of their lobular location, were similar in the following respects: glycogen content, total area of rough-surfaced endoplasmic reticulum, total area of mitochondrial envelope, size of peroxisomes, and the 2:1 ratio of numbers of mitochondria and peroxisomes. Furthermore, despite a large variation in the size and shape of mitochondria, their internal composition was shown to be remarkably constant with respect to matrix volume, area of cristae membrane, and numbers of dense granules per unit volume. These observations suggest that quantitative structural analysis is not merely an aid to morphological description, but is also a technique which can reveal heretofore unknown and unsuspected relationships.

The generous and helpful encouragement given by Drs. D. Spiro and J. Wiener is gratefully acknowledged. It is also a privilege to commend the technical assistance of Miss B. M. Shiner, Miss F. Liu, Mr. C. B. Canson, Mr. M. Rosen, and Mr. L. W. Koster.

This study was supported in part by the General Research Support Grant and Grant HE-5906 of the United States Public Health Service.

This work was presented in part at the 6th Annual Meeting of the American Society for Cell Biology (55) on November 18, 1966.

Received for publication 28 July 1967, and in revised form 4 December 1967.

REFERENCES

1. NOVIKOFF, A. B., and E. ESSNER. 1960. The liver cell. Some new approaches to its study. *Am. J. Med.* **29**:102.
2. ROUILLER, C., and A. M. JEZEQUEL. 1963. Electron microscopy of the liver. *In* The Liver. C. Rouiller, editor. Academic Press Inc., New York. **1**:195.
3. DAVID, H. 1964. Submicroscopic Ortho-and Patho-Morphology of the Liver. The MacMillan Co., New York.
4. BRUNI, C., and K. R. PORTER. 1965. The fine structure of the parenchymal cell of the normal rat liver. I. General observations. *Am. J. Pathol.* **46**:691.
5. LEHNINGER, A. L. 1964. The Mitochondrion. W. A. Benjamin, Inc., New York.
6. ROODYN, D. B. 1965. The classification and partial tabulation of enzyme studies on subcellular fractions isolated by differential centrifuging. *Intern. Rev. Cytol.* **18**:99.
7. DE DUVE, C., and P. BAUDHUIN. 1966. Peroxisomes (microbodies and related particles). *Physiol. Rev.* **46**:323.
8. DE DUVE, C., and R. WATTIAUX. 1966. Functions of lysosomes. *Ann. Rev. Physiol.* **28**:435.
9. GAHAN, P. B. 1967. Histochemistry of lysosomes. *Intern. Rev. Cytol.* **21**:2.
10. NOEL, R. 1923. Recherches histo-physiologiques sur la cellule hépatique des mammifères. *Arch. anat. microscop.* **19**:1.
11. NOVIKOFF, A. B. 1961. Mitochondria (Chondriosomes). *In* The Cell. J. Brachet and A. E. Mirsky, editors. Academic Press Inc., New York. **2**:299.
12. DEANE, H. W. 1944. A cytological study of the diurnal cycle of the liver of the mouse in relation to storage and secretion. *Anat. Record.* **88**:39.
13. NOVIKOFF, A. B. 1959. Cell heterogeneity within the hepatic lobule of the rat (staining reaction). *J. Histochem. Cytochem.* **7**:240.
14. WACHSTEIN, M. 1963. Cyto- and histochemistry of the liver. *In* The Liver. C. Rouiller, editor. Academic Press Inc., New York. **1**:137.
15. REYNOLDS, E. S. 1963. Liver parenchymal cell injury. I. Initial alterations of the cell following poisoning with carbon tetrachloride. *J. Cell Biol.* **19**:139.
16. REMMER, H., and H. J. MERKER. 1963. Enzyminduktion und Vermehrung von endoplasmatischen Retikulum in der Leberzelle wahrend der Behandlung mit Phenobarbital. *Klin. Wochschr.* **41**:276.
17. STEINER, J. W., M. J. PHILLIPS, and K. MIYAI. 1964. Ultrastructural and subcellular pathology of the liver. *Intern. Rev. Exptl. Pathol.* **3**:66.
18. BURGER, P. C., and P. B. HERDSON. 1966. Phenobarbital-induced fine structural changes in rat liver. *Am. J. Pathol.* **48**:793.
19. SAFRAN, A. P., and F. SCHAFFNER. 1967. Chronic passive congestion of the liver in man. *Am. J. Pathol.* **50**:447.
20. WEIBEL, E. R., and H. ELIAS. 1967. Quantitative Methods in Morphology. E. R. Weibel and H. Elias, editors. Springer-Verlag. Berlin-Heidelberg-New York.
21. STRIEBICH, M. J., E. SHELTON, and W. C. SCHNEIDER. 1953. Quantitative morphological studies on the livers and liver homogenates of rats fed 2-methyl- or 3′-methyl-4-dimethylaminoazobenzene. *Cancer Res.* **13**:279.
22. CARPENTER, A. M. 1966. Scanning methods: Volume quantitation of tissues, cells and subcellular components. *J. Histochem. Cytochem.* **14**:834.
23. DAOUST, R. 1958. The cell population of liver tissue and the cytological reference bases. *In* Liver Function. R. W. Brauer, editor. American Institute of Biological Sciences. Publication **4**:3.
24. LOUD, A. V. 1962. A method for the quantitative estimation of cytoplasmic structures. *J. Cell Biol.* **15**:481.
25. LOUD, A. V., W. C. BARANY, and B. A. PACK. 1965. Quantitative evaluation of cytoplasmic structures in electron micrographs. *Lab. Invest.* **14**:996.
26. WIENER, J., A. V. LOUD, D. V. KIMBERG, and D. SPIRO. 1968. A quantitative description of cortisone-induced alterations in the ultrastructure of rat liver parenchymal cells. **37**:47.
27. KIMBERG, D. V., A. V. LOUD, and J. WIENER. 1968. Cortisone-induced alterations in mitochondrial function and structure. **37**:63.
28. KOSTER, L. W., and D. SPIRO. 1963. The substitution of sheet film for glass plates in electron microscopy. *J. Biol. Phot. Assoc.* **31**:49.
29. BAHR, G. F., and E. ZEITLER. 1965. The determination of magnification in the electron

microscope. II. Means for the determination of magnification. *Lab. Invest.* **14**:880.

30. WEIBEL, E. R., G. S. KISTLER, and W. F. SCHERLE. 1966. Practical stereological methods for morphometric cytology. *J. Cell Biol.* **30**:23.
31. DELESSE, M. A. 1847. Procédé mécanique pour déterminer la composition des roches. *Compt. rend. Acad. Sci.* **25**:544.
32. ROSIWAL, A. 1898. Ueber geometrische Gesteinsanalysen. Ein einfacher Weg zur ziffermässigen Feststellung des Quantitätsverhaltnisses der Mineralbestandteile gemengter Gesteine. Verhandlungen der Kaiserliche-Konigliche Geologische Reichsanstalt, Vienna **6**:143.
33. GLAGOLEV, A. A. 1933. On the geometrical methods of quantitative mineralogic analysis of rocks. Transactions of the Institute of Economic Minerology and Metallurgy. Moscow. No. 59.
34. TOMKEIEFF, S. I. 1945. Linear intercepts, areas and volumes. *Nature.* **155**:24.
35. SMITH, C. S., and L. GUTTMAN. 1953. Measurement of internal boundaries in three-dimensional structures by random sectioning. *J. Metals.* **5**:81.
36. DEHOFF, R. T., and F. N. RHINES. 1961. Determination of the number of particles per unit volume from measurements made on random plane sections: the general cylinder and the ellipsoid. *Tr. AIME.* **221**:975.
37. ELIAS, H., A. HENNIG, and P. M. ELIAS. 1961. Some methods for the study of kidney structure. *Z. wissensch. Mikroskop.* **65**:70.
38. FLODERUS, S. 1944. Untersuchungen über den Bau der menschlichen Hypophyse mit besonderer Berücksichtigung der quantitativen mikromorphologischen Verhältnisse. *Acta Pathol. Microbiol. Scand.* Suppl. 53.
39. HAUG, H. 1967. Problems und Methoden der Strukturzählung im Schnittpräparat. *In* Quantitative Methods in Morphology. E. R. Weibel and H. Elias, editors. Springer-Verlag. Berlin-Heidelberg-New York.
40. SEHAUD, J., A. RYTER, and E. KELLENBERGER. 1959. Considerations quantitatives sur des coupes ultraminces de bacteries infectees par un bacteriophage. *J. Biophys. Biochem. Cytol.* **5**:469.
41. ZELANDER, T., and R. EKHOLM. 1960. Determination of the thickness of electron microscopy sections. *J. Ultrastruct. Res.* **4**:413.
42. WEIBEL, E. R., and D. M. GOMEZ. 1962. A principle for counting tissue structures on random sections. *J. Appl. Physiol.* **17**:343.
43. HENNIG, A., and J. R. MEYER-ARENDT. 1963. Microscopic volume determination and probability. *Lab. Invest.* **12**:460.
44. HENNIG, A. 1959. A critical survey of volume and surface measurement in microscopy. *Zeiss Werkzeitschrift.* No. 30.
45. BACH, G. 1964. Bestimmung der Häufigkeitsverteilung der Radien kugelförmiger Partikel aus den Häufigkeiten ihrer Schnittkreise in zufälligen Schnitten der Dicke δ. *Z. wissensch. Mikroskop.* **66**:193.
46. BACH, G. 1967. Kugelgrössenverteilung und Verteilung der Schnittkreise; ihre wechselseitigen Beziehungen und Verfahren zur Bestimmung der einen aus der anderen. *In* Quantitative Methods in Morphology. E. R. Weibel and H. Elias, editors. Springer-Verlag. Berlin-Heidelberg-New York.
47. ST. AUBIN, P. M. G., and N. L. R. BUCHER. 1952. A study of binucleate cell counts in resting and regenerating rat liver employing a mechanical method for the separation of liver cells. *Anat. Record.* **112**:797.
48. ELIAS, H. 1955. Liver morphology. *Biol. Rev.* **30**:263.
49. REVEL, J. P. 1964. Electron microscopy of glycogen. *J. Histochem. Cytochem.* **12**:104.
50. WILLIAMS, R. C., and F. KALLMAN. 1955. Interpretations of electron micrographs of single and serial sections. *J. Biophys. Biochem. Cytol.* **1**:301.
51. LOUD, A. V. 1967. Quantitative estimation of the loss of membrane images resulting from oblique sectioning of biological membranes. *In* Proceedings 25th Anniversary Meeting of Electron Microscopy Society of America, C. J. Arceneaux, editor. Claitor's Book Store, Baton Rouge, La. 144.
52. NOVIKOFF, A. B., and W. Y. SHIN. 1964. The endoplasmic reticulum in the Golgi zone and its relations to microbodies, Golgi apparatus and autophagic vacuoles in rat liver cells. *J. Microscop.* **3**:187.
53. ERICSSON, J. L. E., and W. H. GLINSMANN. 1966. Observations on the subcellular organization of hepatic parenchymal cells. I. Golgi apparatus, cytosomes and cytosegresomes in normal cells. *Lab. Invest.* **15**:750.
54. LOUD, A. V. 1967. Ultrastructural equilibria in liver cell cytoplasm. *In* Proceedings 2nd International Congress for Stereology. H. Elias, editor. Springer-Verlag, New York. 72.
55. LOUD, A. V. 1966. Quantitative electron microscopy of the rat liver lobule. *J. Cell Biol.* **31**:69A.